

## RAW GAS PARTICLES AND DEPOSITIONS IN FUME TREATMENT FACILITIES IN ALUMINIUM SMELTING

Heiko Gaertner<sup>1</sup>, Arne Petter Ratvik<sup>2</sup>, and Thor Anders Aarhaug<sup>2</sup>

<sup>1</sup>NTNU Department of Materials Science and Engineering, NO-7491 Trondheim, Norway

<sup>2</sup>SINTEF Materials and Chemistry, NO-7465 Trondheim, Norway

Keywords: Aluminium electrolysis, Particulate emissions, Pot Raw-gas, Particle distribution, Impurities, Scale

### Abstract

The trace element distributions in depositions found in the gas treatment centres (GTCs) exhibit striking similarities with the coarse pot gas particulates captured in a standard cyclone. To gain a better understanding of possible scale formation mechanisms and components involved, several analysis techniques were applied and compared. Pot exhaust coarse and fine particles, as well as scale samples collected from the gas treatment centre of the same Al-smelter were evaluated. LECO and Sintaszyzer results, XRD, IR spectra and XPS pattern of grey scale samples and raw gas particle fractions are presented. Recrystallization of sodium fluoroaluminates due to HF adsorption reactions in combination with moisture is suggested as one formation mechanism.

### Introduction

In dry cleaning of pot exhaust, expensive fluorides are captured and returned to the production. At the same time impurities are accumulated in the finer fractions of the secondary alumina [1, 2] that is enriched with fluoride. Metal quality and current efficiency in electrowinning can be improved by removing contaminants from the raw material feedstock. Removal of the fine fraction of the fluoride enriched secondary alumina (with particle sizes usually below 20 to 45  $\mu\text{m}$ ) is a viable method to improve metal quality and cell performance as demonstrated by several authors. Although the particle and impurity distribution in reacted alumina is well known [8, 9, 10, 11, 12], information about the composition of particles in the pot exhaust is not extensive [13, 14]. Most plants have not found removal of impurities profitable while others separate small process streams for deposition or feed primary alumina to improve metal quality [3, 4]. However, shortage of high purity raw materials and strict requirements for metal purity may make the removal of contaminant elements more attractive or even necessary in the future [5, 6, 7].

A variety of trace elements with negative effect on the reduction process are present in the coarse particle fraction of pot exhaust [15]. The impurity content in particulate emissions increased significantly for par-

ticles with  $D_i > 1 \mu\text{m}$ . Maximum impurity concentrations were recorded for fume fractions with particle size  $D_i > 10 \mu\text{m}$ . Up to 2.4 wt% impurities (Ni, Fe, P, V, Ti, Co, Cu, Zn, and Ga) could be obtained in cyclone fractions using an EPA standard cyclone [16] operated with a cut-size of approximately 11  $\mu\text{m}$ . By retaining 14 wt% of the pot exhaust particles in a standard cyclone the content of impurity elements, carbon dust and sulphur were reduced by approximately 24 %, 47 %, and 3.6 %, respectively, while valuable fluorides remain in the process gas. Comparison of impurity concentrations showed striking similarities between coarse pot exhaust particles and grey scale samples [15]. The analysis results support an assumption that the coarse particles from pot exhausts are the main component in depositions found in the pot gas treatment centre. To gain a better understanding of possible mechanisms and components involved in scale formation a comprehensive analysis using several techniques were applied on particulate emissions from pot exhaust, fractions of alumina fines, and samples of scale.

### Experimental

The ISOK4/TPS4 instruments were used to sample pot exhaust from the electrolysis cells. The sampling equipment allowed for sampling of process gases to determine the total dust loads under different operational conditions such as varying temperature and volumetric flow. The experimental set-up is sketched in Figure 1.

The sample flow rate was controlled by the TPS 4 unit (pos. 5 in Figure 1) The equipment used the pressure drop over a calibrated orifice to regulate the frequency controlled gas-tight rotary-vane vacuum pump (pos. 4 in Figure 1). The sample flow was kept in the range of -5 % to +15 % of the preselected. Flow rate as prescribed in EN 13284-1 [17]. Coarse particles were separated from the sample flow with the help of an EPA standard cyclone [16] while fines were collected on a Pall Emfab TX40HI20-WW filter. For the determination of trace element concentrations suitable amounts of particle samples were weighed on a Mettler Toledo XP6U ultra micro-balance and dissolved in  $\text{HNO}_3$  and HF solutions in a MLS Milestone microwave Ultraclave (250 °C at 95 bar) before they were analysed with Thermo Scientific Element 2 high resolution ICP-MS .

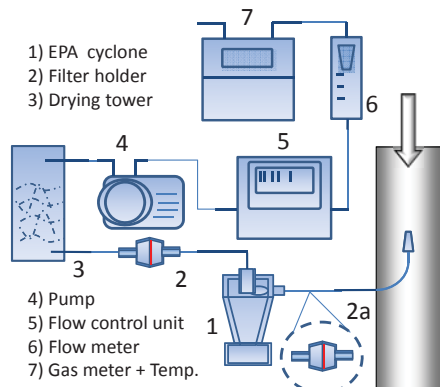


Figure 1: *ISOK<sub>4</sub>/TPS<sub>4</sub> sampling system for isokinetic sampling of pot exhaust particles. Position 2a marks the filter holder position for determination of the total dust load.*

## Results and Discussion

To investigate the influence of water on coarse pot exhaust particles (cyclone samples) four different types of samples were prepared. The “Filter” and “Cyclone” samples consisted of fine and coarse pot exhaust particles collected during the ISOK4 measurement campaigns, while the “Grey scale” samples consisted of crushed grey scale from the gas treatment centre of the same smelter. The “Cyclone + H<sub>2</sub>O” samples were obtained by reacting coarse particles with a drop of distilled water placed on the particles in a Pyrex Petri-dish and dried at 110 °C for 24 h. Loose particles were removed after drying and the fraction that clogged and stuck to the Petri-dish were analysed.

### XRF, LECO, and Sintalyzer Results

In Table I lists the normalized element concentrations recorded with XRF, LECO and Sintalyzer.

LECO<sup>1</sup> and Sintalyzer analysis of three sample parallels show that large amounts of carbon dust concentrate in the coarse pot exhaust particles. Approximately 17 % and 3 % carbon were measured in cyclone and filter samples, respectively. The determined sulphur and potassium and trace-element concentrations presented in Table I are in fair agreement with the ICP-MS analysis results [15]. The general trend shows that trace elements concentrate in the coarse particle fractions and in the scale depositions.

<sup>1</sup>LECO analysis conducted at Hydro Aluminium AS Primary Metal Technology. Highest calibration standard at Hydro was 3,4 % for C and 0,2 % for S, which can lead to deviations due to the high contents in the sample compared to the calibration standards.

Table I: *XRF, LECO and Sintalyzer results normalized to 100 % based on the sum of detectable elements.*

Element %	Scale 1	Cyclone #3 0.5m <sup>3</sup> /h	Cyclone #4 +H <sub>2</sub> O	Filter #43
F	15.97	20.19	19.27	35.30
Na	12.22	10.75	12.51	24.41
Al	58.70	61.97	59.52	31.89
Si	0.10	1.10	0.29	0.46
P	0.35	0.35	0.18	0.18
S	6.54	3.27	4.89	6.47
K	0.77	0.18	0.38	0.55
Ca	0.25	0.89	1.34	0.14
Fe	2.14	0.25	0.41	
Ni	1.77	0.30	0.91	0.09
Cu	0.01	0.08	0.02	
Zn	0.04			0.01
Ga	0.10			
As	0.32			0.25
Mo	0.21			
Pb	0.15			

### LECO

C	2-3.0*	17.0	3.0
S	-	1.4	6.1

### Sintalyzer

F	21.0	29.8
---	------	------

\* private conversation [18]

## IR Results

For further characterization IR-spectroscopy was used in addition to the ICP-MS, XRD and XPS analysis. Filter and cyclone dust as well as crushed grey scale, all with a weight of 1.3 to 2 mg, were mixed with 200 mg KBr and pressed to 13 mmØ discs with a pressure of 100 kN for 2 minutes. The IR-transmittance spectra were recorded in the MIR region, using a Bruker IFS 66v FTIR spectrometer<sup>2</sup>. A spectra consisted of 200 scans in the spectral range 400-4000 cm<sup>-1</sup> with a resolution of 2 cm<sup>-1</sup> corrected for the background.

IR analysis results can be summarised as follows:

- The coarse pot exhaust particles (cyclone samples) showed most similarities with the “Grey Scale” sample. Compared to the Cyclone sample the “Grey Scale” consisted of larger amounts of chiolite with increased alumina content and considerable amounts of sulphur containing compounds. Based on Bondam [19] and Grobelny [20] the differences in the spectra in the region 500 – 800 cm<sup>-1</sup> (area within the red square) the broadened peaks displaced to larger wave numbers are explained by the changing ratios of cryolite, chiolite, and NaAlF<sub>4</sub>. The peak broadening due to absorption in the wavelength region 750 to 570 cm<sup>-1</sup> can be assigned to increasing content of

<sup>2</sup>Bruker IFS 66v FTIR spectrometer: IR source, KBr beam splitter, and DTGS KBr detector for MIR measurements.

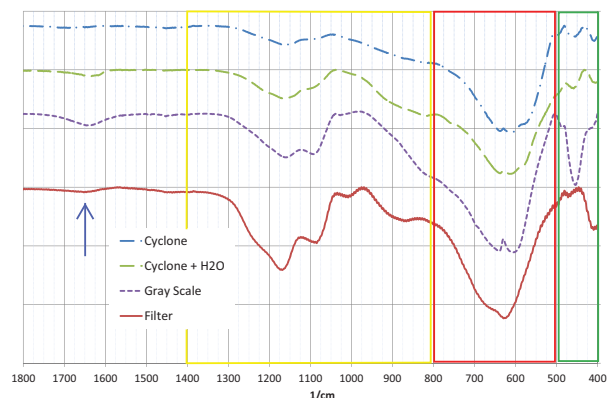


Figure 2: IR-Spectra of pot exhaust particles and grey scale sample. Wave-number  $400 - 1800 \text{ cm}^{-1}$ .

$\text{NaAlF}_4$  as well as a typical feature of  $\text{AlF}_3$ .

- The “Grey Scale” sample showed a significant absorption signal typical for hydroxides (OH-stretching region at approx.  $1640$  and  $3450 \text{ cm}^{-1}$ ). The water adsorption was not as pronounced in the “Cyclone” coarse, but was synthesized by treating cyclone dust with water. The fact that cyclone sample mixed with water and dried at  $100 \text{ }^\circ\text{C}$  is quite similar to the “Grey scale” sample suggests that moisture plays an important role in the scale formation.
- The IR spectra gave strong evidence for the assumption that sulphur is present in the form of sulphates [21]. According to Klopogge et al. [22] the IR absorptions at approximately  $1126$ ,  $614$  and  $982 \text{ cm}^{-1}$  (area marked with yellow square) can be assigned to the  $\nu_3$ ,  $\nu_4$ , and  $\nu_1$  modes characteristic for the  $\text{SO}_4^{2-}$  anion. In the pot exhaust particles, the sulphate content increased significantly with decreasing particle sizes. Considerable amounts of sulphates were also present in the the scale sample.

### XPS Results

Wide-scan survey spectra of filter and cyclone dust as well as crushed grey scale were measured by X-ray photoelectron spectroscopy (XPS). The XPS measurements were performed using a SES2002 electron energy analyser in conjunction with a mono-chromatised  $\text{Al K}\alpha$  ( $h\nu = 1487 \text{ eV}$ ) X-ray source (both Gammatdata-Scienta). A total energy resolution of about  $0.4 \text{ eV}$  could be achieved at pass energy of  $200 \text{ eV}$  in the fixed analyser transmission mode. The X-ray anode was operated at  $250 \text{ W}$ . XPS is a surface chemical analysis technique that gives information about the elemental compositions within the top  $1$  to  $10 \text{ nm}$  of the material. The maximum  $\text{Al}2s$  binding energy (BE) served as a common fixed point to compare relative changes in BE peak positions and intensities. The  $\text{Al}2s$  BE-peak maxima of all scans were fixed to

$-119 \text{ eV}$ , the typical position for  $\text{Al}2s$  binding energy when using an  $\text{Al K}\alpha$  X-ray source. In addition to the off-set correction, the scan’s intensities were scaled to allow for comparison of changes relative to the common  $\text{Al}2s$  peak maximum.

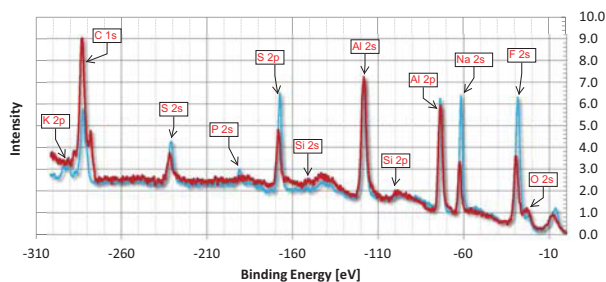


Figure 3: Labelled XPS-scan of filter (blue graph) and grey scale sample (red graph).

In Figure 3 the XPS spectra of a filter and a cyclone sample are labelled with relevant peaks. The intensities recorded in the BE-region typical for F, Na, K, and S were higher in the filter fines than in the scale and cyclone coarse. This suggested that the scanned surface of the filter fines contained significantly more Na and F (relative to the amount of Al) than the coarse particle fraction represented by the cyclone sample. This is also in accordance with the Sintalyzer and EDS analysis. With the ICP-MS, IR and XRD analysis phosphorous was previously not detected in significant amounts in the fines. However, XPS scans detected phosphorous on the surface of the filter sample.

With respect to relative intensities and binding energy distribution, the composition of the surface layers of the cyclone samples (Figure 4(b)) was most similar to that of the grey scale sample (Figure 4(a)). Filter fines contained larger amounts of sodium and fluoride relative to the content of aluminium due to  $\text{NaAlF}_4$  and  $\text{Na}_5\text{Al}_3\text{F}_{14}$ , while the coarse particles contained larger amounts of oxygen, presumably in the form of  $\text{Al}_2\text{O}_3$ .

The findings based on XPS scans can be summarized as follows:

- The XPS scans of filter-samples representing the particles with diameters  $D_{50} < 10 \text{ }\mu\text{m}$  were significantly different from the cyclone and grey scale samples. The fines showed a lower intensity of oxygen but significantly higher intensities for Na and F compared to the coarser samples.
- Phosphorus was detected on the surface of particles in the filter fines. Presumably phosphorus condenses as a thin layer, since the levels recorded in the same fraction with ICP-MS were usually low ( $120\text{--}400 \text{ ppm}$  in filter fines and  $1000 \text{ ppm}$  in the cyclone fractions).
- The sulphur binding energy pattern was found in all samples showing that the element was present in all

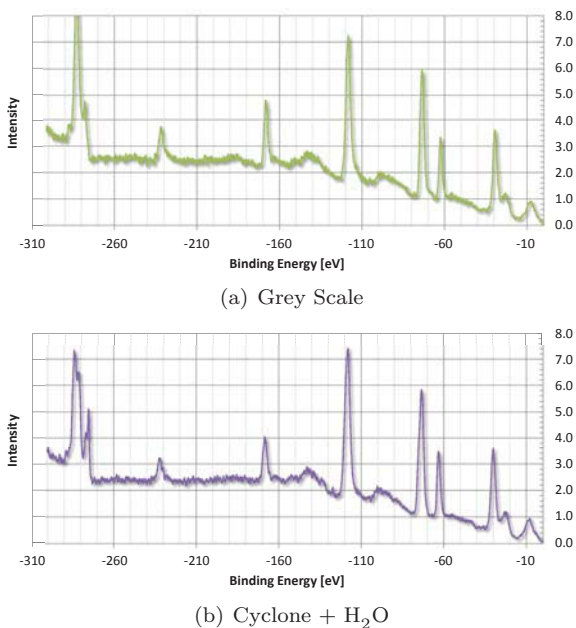


Figure 4: Scaled XPS scans: Grey scale (a) and cyclone sample (b).

samples. A higher sulphur content was recorded in the fines as already shown by the HR ICP-MS analysis [15]. Differentiation of sulphur compounds based on the present XPS scans was difficult due to noise and low resolution. However, investigation of sulphur species in the pot exhaust should be subject to further research since significant amounts of sulphur are detected in the scale samples.

- Binding energies in the carbon region C1s (usually at -287 eV) were significantly different for all samples. Cyclone samples contained particles with binding energies also present in the scale sample but not all carbon containing compounds found in the cyclone sample seemed to be present in the grey scale.
- The Cyclone sample represents the coarse particle fraction with  $D_{50} > 10 \mu\text{m}$  in the pot exhaust. These coarse particles had quite similar XPS-patterns to the “Grey Scale” sample.

### XRD Results

A Bruker AXS D8-Focus diffractometer operated with a Cu K $\alpha$  source and Lynx Eye detector was used for the XRD measurements. Although coarse pot exhaust particles and grey scale samples showed similar chemical composition, the XRD analysis revealed significant differences in crystal structure. In Figure 5 XRD-patterns of pot exhaust fines and coarse fractions are compared to a grey scale sample. Besides chiolite (PDF: 30-1144) and cryolite (PDF:25-0772), the NaAlF<sub>4</sub> pattern (PDF:

51-1675) was the most distinct in the filter particles. The coarse fraction represented by the cyclone samples contained NaAlF<sub>4</sub> together with significant amounts of cryolite, chiolite, corundum (PDF: 10-0173) and most probably aluminium fluoride (PDF: 44-0231). The distinct cryolite XRD-pattern, observable in the coarse particle fractions, was not visible in the grey scale sample, while the chiolite and NaAlF<sub>4</sub> peaks were broadened. This observation is interpreted as recrystallization of sodium fluoroaluminates during scale formation as observed by Grobelny [23, 20].

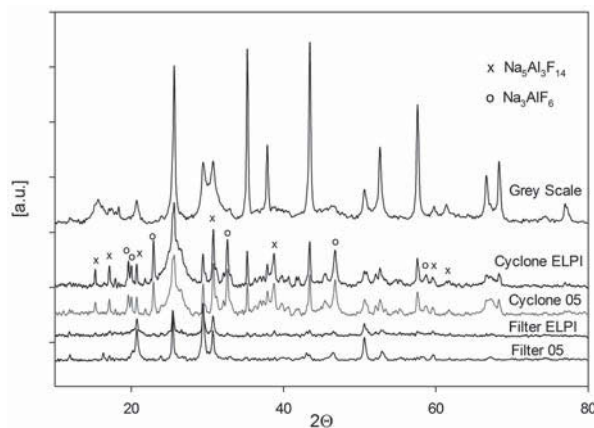


Figure 5: XRD analysis results of different particle fractions in raw gas from aluminium electrolysis cells. Bottom to top: Two filter samples followed by two cyclone samples consisting of particles collected in a cyclone operated with a flow rate of 0.5 m<sup>3</sup>/h (cut-size  $D_{50} = 9.86 \mu\text{m}$ ). The scan on top is from a grey scale sample.

Grobelny investigated the formation of sodium fluoroaluminates by heating of AlF<sub>3</sub> solutions<sup>3</sup> with additions of crystalline sodium fluoride and cryolite. At temperatures of 80 to 100 °C. The author observed the formation of NaAlF<sub>4</sub> · H<sub>2</sub>O and/or Na<sub>5</sub>Al<sub>3</sub>F<sub>14</sub> as final products when reacting equimolar amounts of AlF<sub>3</sub> and NaF after some Na<sub>3</sub>AlF<sub>6</sub> was initially formed. Lower temperatures (60 °C) yielded chiolite and cryolite, while higher temperatures favoured the formation of NaAlF<sub>4</sub> · H<sub>2</sub>O. The layer like structure and the disappearance of cryolite in the grey scale sample suggest that scale may form by recrystallization of sodium fluoroaluminates as reaction to cyclic changes in water content in the gas treatment facilities. Dependent on the storage conditions, the alumina introduces moisture into the dry-scrubber either in the form of aluminium hydroxides (Equation 1) or loosely bound surface water [24], while HF from the pot exhaust can react with fume components and alumina to form AlF<sub>3</sub>.

<sup>3</sup>Solutions with 21 and 75 g/l AlF<sub>3</sub> having pH values adjusted to 1.2 and 2.8 with the help of fluorosilicic acid H<sub>2</sub>SiF<sub>6</sub> 10 g/l.



Aluminium fluoride solutions can form when water vapours condense on fine particles leading to hydrolysis and recrystallization of deposited pot exhaust particles. Thus, recrystallization of cryolite in the presence of chiolite and  $NaAlF_4$  nuclei is thought to be a possible scale formation mechanism. To test this assumption particle samples from pot exhaust were reacted with water and  $AlF_3$ -solutions.

### Moisture - Recrystallization

In Figure 6 coarse pot exhaust particles and grey scale are compared to particles reacted with  $AlF_3$  solution. The addition of distilled water to cyclone dust and subsequent drying did not alter the crystal structure. Treatment of the combined sample with an  $AlF_3$  solution<sup>4</sup> at 110 °C in the drying cabinet led to weakened cryolite and  $NaAlF_4$  signals as shown in Figure 6. In the “Cycl+ $AlF_3$ -sol-Li” sample the intensity of the cryolite diffraction pattern was weakened relative to the cryolite intensity. This observation suggests that cryolite is transformed to chiolite in the presence of  $AlF_3$  solutions at temperatures prevailing in dry scrubbers.

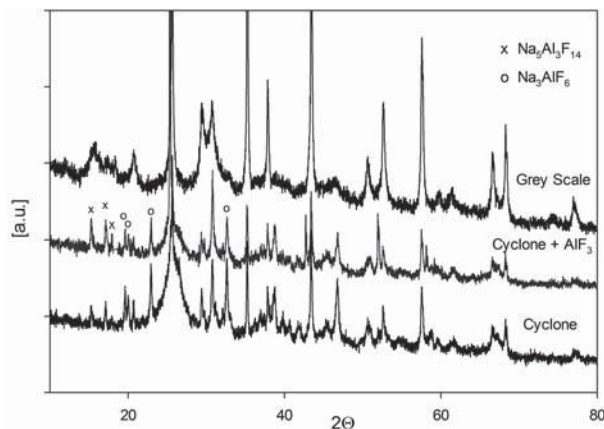


Figure 6: XRD-scans of pot exhaust particles as collected in standard cyclone, reacted with  $AlF_3$  solution (Peak for lithium compound contamination removed) and grey scale sample.

However, the analysed data does not allow a firm conclusion with regard to the reaction mechanisms for the formation of scale, since an attempt to reproduce and enhance the recrystallization yielded a different crystal structure (Figure 7). The contact of pot exhaust particles with  $D_1 > 10 \mu m$  with saturated  $AlF_3$  solution ( $AlF_3$  crystal added to dust with drop-wise addition of solution over an extended period of time at 110 °C in a closed

<sup>4</sup> $AlF_3$  solution added drop wise in 40 min. intervals over a period of approximately 8 hours

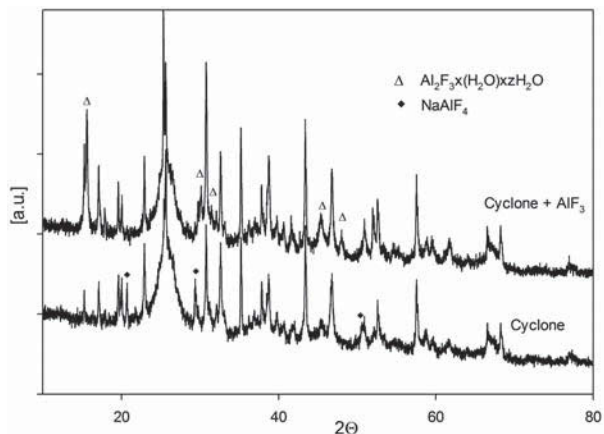


Figure 7: Aluminium hydroxide fluoride hydrate formation after contact with saturated aluminium fluoride solution over several hours.

petri-dish) led to the formation of aluminium fluoride hydrate (PDF:01-074-0940) while the  $NaAlF_4$  pattern disappeared.

### Summary and Concluding Remarks

Coarse particles in the pot exhaust have a similar composition to scale samples and thus, are considered as one of the main components in depositions found in dry-scrubber facilities. Phosphorus condensates were detected on the surfaces of particles in the filter fines. Sulphur was present in the form of sulphates. Considerable amounts of sulphates were also present in the scale sample. Not all carbon containing compounds found in the coarse pot exhaust particles seem to be present in the grey scale. The grey scale sample showed IR absorption patterns in the OH-stretching region typical for water. Cyclone dust treated with water support the assumption that moisture plays an important role during scale formation. Recrystallization processes were observed in XRD when  $AlF_3$ -solution was added to cyclone dust at 110 °C. The fact that cryolite and  $NaAlF_4$  can be recrystallized in short term experiments is support for the assumption that recrystallization can be a mechanism for scale formation in fume treatment facilities. The fact that modifications during the experiments led to different results suggests that the recrystallisation varies with the actual conditions. The extent of the work related to scale formation does not allow a firm conclusion about the conditions favouring scale formation. Thus, the recrystallization of coarse pot exhaust particles as a possible scale formation mechanism initiated by moisture and  $AlF_3$  should be subject to further investigations.

## Acknowledgments

This study is a part of the ROMA research project with financial support of the Research Council of Norway and Norwegian aluminium and metallurgical industry. The support of operators, engineers and professionals at NTNU and Hydro Aluminium smelters is thankfully acknowledged. ICPMS analysis was performed by Overingenir Syverin Lierhagen at the Department of Chemistry, NTNU. XPS scans were performed by Professor Steinar Raaen at the Department of Physics at NTNU. The support of Professor Mari-Ann Einarsrud and Dr. Tobias Danner at the Department of Materials Science and Engineering during IR analysis is thankfully acknowledged. XRF and LECO analysis was performed by Kari Bolstad under supervision of Kristin Gulbrandsen and Dr.ing. Lorentz Petter Lossius, Principal Engineer at Primary Metal Technology (PMT), Hydro Årdal.

## References

- [1] V. Sparwald, "Beitrag zur Verflchtigung der Begleitelemente bei der Aluminium-Schmelzflusselektrolyse," *Erzmetall*, vol. (26) Heft 11, pp. 529–578, (1973).
- [2] E. Böhm and L. Reh, "Removal of impurities in aluminum smelter dry gas using the VAW–Lurgi process," *Light Metals*, vol. 2, pp. 509–525, (1976).
- [3] L.C.B. Martins, "Use of dry scrubber primary cyclone to improve the purity of al," *Light Metals*, pp. 315–317, (1987).
- [4] D.R. Augood, "Impurity distributions in alumina reduction plants," *Light Metals*, pp. 413–427, (1980).
- [5] S.J. Lindsay and N.R. Dando, "Dry scrubbing for modern pre-bake cells," *Light Metals*, pp. 275–280, (2009).
- [6] S.J. Lindsay, "Raw material impurities and the challenge ahead," *Light Metals*, pp. 5–8, (2013).
- [7] J.B. Metson, D.S. Wong, J.H. Hung, and M.P. Taylor, "Impacts of impurities introduced into the aluminium reduction cell," *Light Metals*, pp. 9–13, (2013).
- [8] E. Cutshall, "Removal of phosphorus from dry scrubber alumina," *Light Metals*, pp. 927–933, (1979).
- [9] L. Lossius and H.A. Øye, "Removing impurities from secondary alumina fines," *Light Metals*, pp. 249–258, (1992).
- [10] L. Schuh and G. Wedde, "Removal of impurities from dry scrubbed fluoride enriched alumina," *Light Metals*, pp. 399–403, (1996).
- [11] E. Sturm and G. Wedde, "Removing impurities from the aluminium electrolysis process," *Light Metals*, pp. 235–240, (1998).
- [12] G. Gurnon and W. Minchin, "Removal of carbonaceous material from dry scrubber catch in v.s. cell systems," *Light Metals*, vol. 2, pp. 543–552, (1976).
- [13] L. Less and J. Waddington, "The characterisation of aluminium reduction cell fume," *Light Metals*, pp. 499–508, (1971).
- [14] J. Thonstad, F. Nordmo, S. Rolseth, and J.B. Paulsen, "On the transfer of some trace elements in the dry scrubbing systems," *Light Metals*, vol. 2, pp. 463–479, (1978).
- [15] H. Gaertner, A.P. Ratvik, and T.A. Aarhaug, "Trace element concentration in particulates from pot exhausts and depositions in fume treatment facilities," *Light Metals*, pp. 769–774, (2013).
- [16] U. Environmental Protection Agency, "Methods for Measurement of Filterable PM10 and PM2.5 and Measurement of Condensable PM Emissions from Stationary Sources," *EPA, US Environmental Protection Agency, EPA-HQ-OAR-2008-0348 FRL-9236-2*, (2010).
- [17] CEN, "EN 13284-1: Stationary source emissions-Determination of low range mass concentration of dust-Part 1: Manual gravimetric method," *European Committee for Standardization*, (2001).
- [18] M. Isaksen, Hydro Aluminium, Porsgrunn, Norway. "Impurities in raw gas particles and depositions in FTC," *Private conversation*, (2012).
- [19] J. Bondam, "The infrared absorption spectra of a number of sodium fluoroaluminates in the wavenumber region between 500 and 800  $\text{cm}^{-1}$ ," *Acta Chemica Scandinavica*, vol. 25, pp. 3271–3276, (1971).
- [20] M. Grobelny, "The reaction of aluminum fluoride solution with cryolite," *Journal of Fluorine Chemistry*, vol. 8, pp. 353–368, (1976).
- [21] J. Gadsden, *Infrared spectra of minerals and related inorganic compounds*. The Butterworth & Co (Publishers) Ltd, (1975).
- [22] J. Klopogge, D. Wharton, L. Hickey, and R.L. Frost, "Infrared and Raman study of interlayer anions  $\text{CO}_3^{2-}$ ,  $\text{NO}_3^-$ ,  $\text{SO}_4^{2-}$ , and  $\text{ClO}_4^-$  in Mg/Al-hydrotralcite," *American Mineralogist*, vol. 87, no. 5-6, pp. 623–629, (2002).
- [23] M. Grobelny, "Sodium fluoroaluminates formed in the reaction between aluminum fluoride solution and crystalline sodium fluoride," *Journal of Fluorine Chemistry*, vol. 8, pp. 133–144, (1976).
- [24] C. Sommerseth, K.S. Osen, C. Rosenkilde, A.J. Meyer, L.T. Kristiansen, and T.A. Aarhaug, "A method for comparing the HF formation potential of aluminas with different water contents," *Light Metals*, pp. 827–832, (2012).